Microscopic theory of hot-carrier relaxation in semiconductor-based quantum-cascade lasers

Microscopic theory of hot-carrier relaxation in semiconductor-based quantum-cascade lasers

Rita C. Iotti and Fausto Rossi

Citation: Appl. Phys. Lett. **76**, 2265 (2000); doi: 10.1063/1.126316
View online: http://dx.doi.org/10.1063/1.126316
View Table of Contents: http://apl.aip.org/resource/1/APPLAB/v76/i16
Published by the American Institute of Physics.

Microscopic theory of hot-carrier relaxation in semiconductor-based quantum-cascade lasers

Rita C. Iotti[a] and Fausto Rossi
Instituto Nazionale per la Fisica della Materia (INFM) and Dipartimento di Fisica, Politecnico di Torino, Corso Duca degli Abruzzi 24, 10129 Torino, Italy

(Received 12 October 1999; accepted for publication 22 February 2000)

A microscopic analysis of basic nonequilibrium phenomena in unipolar quantum devices is presented. In particular, energy-relaxation processes governing the hot-carrier dynamics in the active region of GaAs-based quantum-cascade lasers are investigated by means of a generalized ensemble Monte Carlo simulation. Such analysis is essential in determining the validity range and limitations of purely macroscopic models with respect to basic device parameters, like injection current and temperature. © *2000 American Institute of Physics.* [S0003-6951(00)01516-3]

Semiconductor-based nanostructures have been the subject of impressive research activity owing to their great flexibility as model systems for basic research[1] as well as effective ''building blocks'' in modern solid-state optoelectronics.[2] Among the most successful applications one must mention a variety of photodetectors[3] as well as unipolar semiconductor lasers.[4] The principle of operation for most of these solid-state devices involves nonequilibrium carrier dynamics between propagating and localized states.[5] In turn, this dynamic is strongly influenced by both intra- and intersubband phonon scattering as well as by carrier concentration and temperature.

Unipolar coherent-light sources like quantum-cascade lasers (QCLs), are usually modeled in terms of three-level systems.[6] Their theoretical description is thus often grounded on purely macroscopic models; the only relevant physical quantities are various carrier concentrations (n_ν) within the different energy levels (ν=1,2,3), whose time evaluation is dictated by the following set of coupled rate equations:

$$\frac{dn_\nu}{dt}=(\alpha_\nu-\beta_\nu n_\nu)_{i/l}+\sum_{\nu'}(n_{\nu'}w_{\nu'\nu}-n_\nu w_{\nu\nu'})_s. \tag{1}$$

This is the sum of the injection/loss (i/l) contribution—α_ν and β_ν being, respectively, the carrier injection and loss rates for level ν—plus the interlevel-scattering (s) term— $w_{\nu\nu'}$ denoting phenomenological scattering rates connecting levels ν and ν'. Such physical parameters are unavoidably global or macroscopic quantities, i.e., their microscopic evaluation would require the knowledge of the carrier distribution function over the whole three-dimensional (3D) $\mathbf{k}$ space.

The aim of this letter is to show that such a macroscopic modeling can only operate as a fitting procedure. The best-fit phenomenological parameters obtained through a comparison with experiments depend strongly on details of the 3D hot-carrier distribution and therefore on the device operation conditions. In order to study the validity range of the macroscopic model in Eq. (1), we shall compare it to a fully kinetic or Boltzmann-like formulation. To this end, the most commonly used approach is the Monte Carlo (MC) method.[7] This has proven a very powerful technique allowing the inclusion, at a kinetic level, of a large variety of scattering mechanisms.

In this letter we shall focus on the hot-carrier dynamics within the active region of QCL devices. To this end we shall employ a fully 3D description of energy relaxation based on microscopic intra- as well as interminiband scattering mechanisms.[5] Within the proposed approach, the time evolution of the carrier distribution function $f_{\mathbf{k}\nu}$ is governed by the following set of Boltzmann-like equations:

$$\frac{d}{dt}f_{\mathbf{k}\nu}=[g_{\mathbf{k}\nu}-\Gamma_{\mathbf{k}\nu}f_{\mathbf{k}\nu}]_{i/l}+\sum_{\mathbf{k}'\nu'}[f_{\mathbf{k}'\nu'}P_{\mathbf{k}'\nu',\mathbf{k}\nu}(1-f_{\mathbf{k}\nu}) - f_{\mathbf{k}\nu}P_{\mathbf{k}\nu,\mathbf{k}'\nu'}(1-f_{\mathbf{k}'\nu'})]_s. \tag{2}$$

The first two terms describe injection and loss of carriers with wave vector $\mathbf{k}$ in miniband ν, while the last one describes in- and out-scattering processes between states $\mathbf{k}\nu$ and $\mathbf{k}'\nu'$. Compared to the macroscopic model in Eq. (1), the present formulation provides a description of hot-carrier intra- and interminiband scattering in terms of microscopic ingredients only. The injection/loss contributions in Eq. (2) are still treated on a partially phenomenological level; however, the injection and loss functions (g and Γ) are now defined within the same kinetic picture $\mathbf{k}\nu$. In view of their Boltzmann-like structures, the above kinetic equations are ''sampled'' by means of a proper MC simulation scheme; Compared to conventional ensemble MC techniques,[7] the actual problem requires a MC simulation where the total number of particles (in the active region of the device) is not constant; to overcome this limitation a combined—direct plus MC—time-dependent solution has been implemented.[8]

In view of the relatively low carrier density (in the range 10^9-10^{11} cm^{-2}) and impurity concentration as well as of the quasiresonant nature of intersubband carrier-longitudinal-optical (LO) phonon scattering in QCL structures,[9] the only interaction mechanism considered in our simulated experiments is carrier-LO phonon scattering. All elastic and quasielastic processes, e.g., ionized impurities, acoustic phonons, and carrier-carrier scattering, will affect the carrier dynamics on a much longer time scale.

[a]Also at: Scuola Normale Superiore, Piazza dei Cavalieri 7, 56126 Pisa, Italy; electronic mail: iotti@athena.polito.it

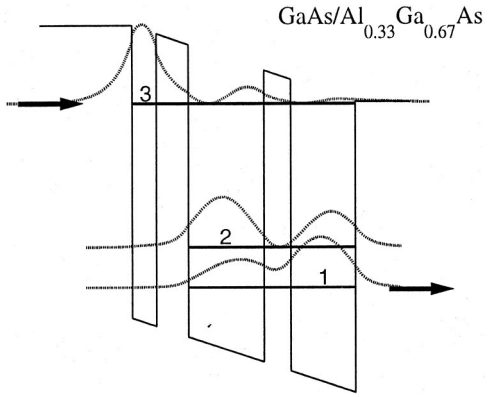

FIG. 1. Schematic representation of the conduction-band profile in the active region of the diagonal-configuration QCL structure of Ref. 9. The levels $\nu=1,2,3$ involved in the simulation, together with the corresponding probability densities, are also plotted.

The proposed simulation scheme has been applied to the diagonal-configuration QCL of Ref. 9, which is schematically depicted in Fig. 1.[10] The 3D single-particle electron states forming the basis set of our scattering dynamics (see their wave function profiles in Fig. 1) are obtained within the standard envelope-function approximation as described in Ref. 5.

Figure 2 shows the three carrier populations ($n_\nu \propto \Sigma_{\mathbf{k}} f_{\mathbf{k}\nu}$) as a function of time for an injection current of 10 kA/ cm^2 at 77 K. At the initial time t_0 the QCL active region is ''empty''; then carriers are continuously injected into level three, according to a Fermi–Dirac distribution corresponding to the lattice temperature and simulated current density, and

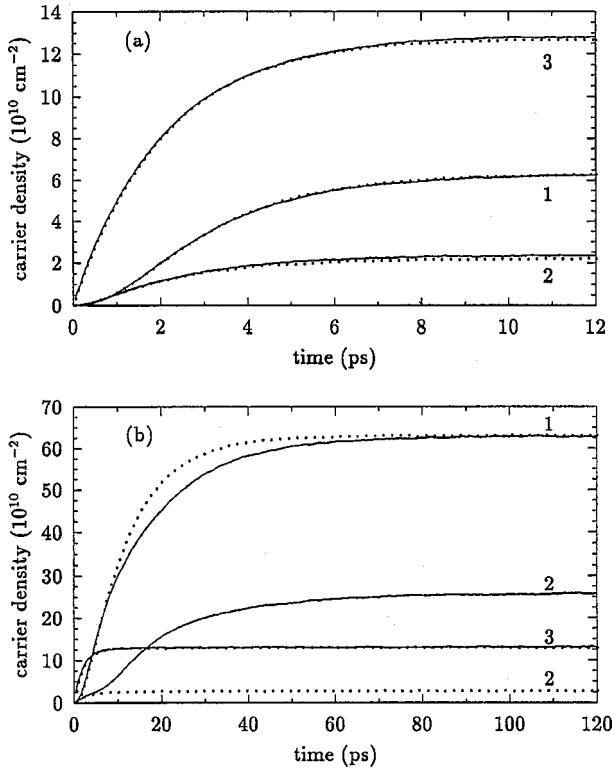

FIG. 2. Various carrier concentrations ($n_\nu, \nu=1,2,3$) as a function of time with (solid) and without (dotted) Pauli-blocking effects. Simulated experiments in (a) and (b) correspond to an escape time from level one of 1 and 10 ps, respectively.

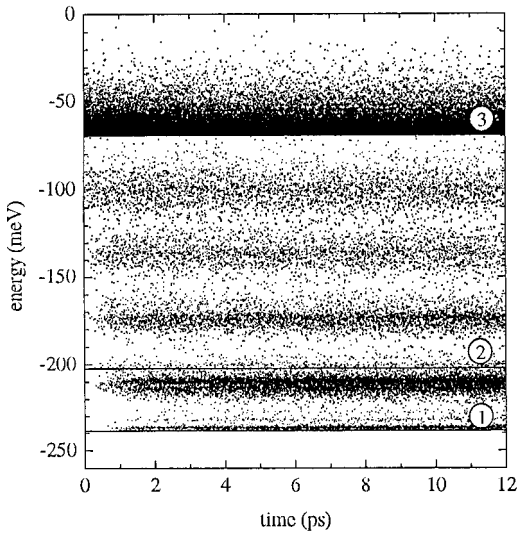

FIG. 3. Energy vs time 2D map of the simulated carriers involved in the $3\rightarrow2\rightarrow1$ cascade process, for the case $\tau_1=1$ ps.

the ''quantum cascade''—$3\rightarrow2$, $2\rightarrow1$—occurs on time scales corresponding to the different values of the interminiband scattering rates. Eventually, the steady-state condition is reached, leading to the desired $3\rightarrow2$ population inversion. Figure 2(a) has been obtained using a typical value for the carrier escape time from level 1: $\tau_1=1/\Gamma_1=1$ps. Here, the results of our MC simulated experiments (solid curves) are compared to the corresponding results obtained by neglecting various Pauli-blocking factors $1-f$ (dotted curves) entering the Boltzmann collision term in Eq. (2). Since in this simulation carrier escape from level one is relatively fast ($\tau_1=1$ ps), we have $f_{\mathbf{k}1}\ll1$ and thus Pauli-blocking effects are not very important. In contrast, by increasing the escape time from level one nonlinear effects due to Pauli blocking may play a crucial role. This can be clearly seen in Fig. 2(b), where the same simulated experiments are shown for $\tau_1=10$ ps. In this case the strong Pauli blocking leads to a significant reduction of the interminiband relaxation $2\rightarrow1$, thus giving rise to a phonon bottleneck and preventing the $3\rightarrow2$ population inversion.[11] Although a quantitative evaluation of carrier dynamics in this regime of slow depletion of level one would require to take into account the competing carrier-carrier scattering channel, Fig. 2(b) shows that, as general prescription, it is important to limit n_1, also if this level is not directly involved in the lasing process. Such Pauli-blocking effects are intrinsically time dependent: During the first stage of the simulation n_1 is still small and the two results (solid and dotted) basically coincide; at later times n_1 increases and significant deviations come into play. As anticipated, such a nonlinear behavior cannot be described by the rate-equation model in Eq. (1). The same is true for the so-called in-plane (or intrasubband) relaxation. This is a purely 3D feature, whose analysis is straightforward within our MC simulation scheme.

Figure 3 presents a direct energy versus time 2D map of the simulated carriers corresponding to the run in Fig. 2(a). We can clearly see that, in addition to the $3\rightarrow2\rightarrow1$ intersubband relaxation—the only one considered in a purely macroscopic model—the quantum-cascade process is also characterized by a significant intrasubband energy relaxation,

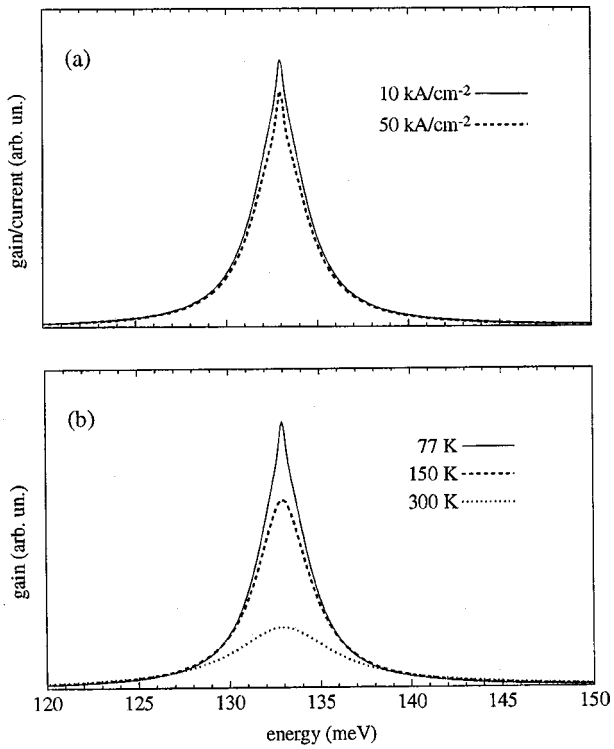

FIG. 4. Intersubband gain spectra as a function of injected current (a), and temperature (b), for the case $\tau_1 = 1$ ps.

resulting in the typical phonon-replica scenario. Since the overall intersubband carrier transfer depends on the scattering rates $P_{\mathbf{k}\nu,\mathbf{k}'\nu'}$ as well as on the carrier distributions $f_{\mathbf{k}\nu}$ in the various subbands [see Eq. (2)], any phenomenological interlevel transition rate $w_{\nu\nu'}$ [see Eq. (1)] is unavoidably time dependent, thus giving rise to nonlinear effects. In particular, for steady-state conditions the energy position of the lowest phonon replica in subband two is crucial in determining the $2\rightarrow1$ phonon-induced carrier transfer.[12] Therefore, in order to improve the QCL performance it is important to locate the phonon replicas in phase-space regions with maximum $2\rightarrow1$ phonon coupling.

Let us now focus on the lasing process in the steady-state regime. Figure 4 presents a collection of gain spectra corresponding to simulated experiments performed under different operation conditions.[13] Figure 4(a) shows simulated gain spectra obtained for two different values of the injection current at a temperature of 77 K. In order to address nonlinear effects, here we plot the ratio between the gain spectrum and the corresponding injection current, which in a purely macroscopic model is current independent. In contrast, our microscopic analysis shows gain suppression which can be ascribed again to Pauli blocking in level one (see Fig. 2). Finally, in Fig. 4(b) we show the gain spectrum as a function of temperature for an injection current of 10 kA/cm^2. At high temperature the $3\rightarrow2$ gain peak is reduced; this is ascribed on the one hand to an increase of the ratio between the $3\rightarrow2$ and $2\rightarrow1$ intersubband scattering rates, and on the other hand to an increase of the spectral linewidth. We stress that this temperature-dependent linewidth is obtained selfconsistently within our kinetic scheme and not simply taken as a phenomenological fitting parameter.

All the results in Fig. 4 clearly show that both injection current and temperature are not dramatically affecting the lasing mechanism within the active region. We can therefore conclude that the absence of gain at high temperatures and currents in state-of-the-art QCL structures[9] should be mainly ascribed to a reduction of quantum efficiency both in the injection/loss tunneling processes and in the active-region/cavity-mode coupling.

We finally come back to the comparison between macroscopic and microscopic modeling: As anticipated, our simulated experiments show significant nonlinear effects, like nonthermal in-plane carrier distribution and Pauli blocking, which cannot be described by the constant-rate dynamics of Eq. (1). This is particularly apparent from the results shown in Figs. 2 and 4.

The authors are grateful to F. Beltram, S. Barbieri, and C. Sirtori for stimulating and fruitful discussions. This work was supported in part by the European Commission through the Brite Euram UNISEL project and the TMR Network ''Ultrafast Quantum Optoelectronics.''

[1] J. Shah, *Ultrafast Spectroscopy of Semiconductors and Semiconductor Nanostructures* (Springer, Berlin, 1996); *Theory of Transport Properties of Semiconductor Nanostructures*, edited by E. Schöll (Chapman and Hall, London, 1998).

[2] *Physics of Quantum Electron Devices*, edited by F. Capasso (Springer, Berlin, 1990).

[3] F. Capasso, W. T. Tsang, and G. F. Williams, IEEE Trans. Electron Devices **ED-30**, 381 (1983); B. F. Levine, J. Appl. Phys. **74**, R1 (1993); S. Barberi, F. Mango, F. Beltram, M. Lazzarino, and L. Sorba Appl. Phys. Lett. **67**, 250 (1995).

[4] J. Faist, F. Capasso, D. L. Sivco, C. Sirtori, and A. Y. Cho, Science **264**, 553 (1994); G. Scamarcio, F. Capasso, C. Sirtori, J. Faist, A. L. Hutchinson, D. L. Sivco, and A. Y. Cho, *ibid.* **276**, 773 (1997); A. Tredicucci, C. Gmachl, F. Capasso, D. L. Sivco, A. L. Hutchinson, and A. Y. Cho, Nature **396**, 350 (1998).

[5] S. Barberi, F. Beltram, and F. Rossi, Phys. Rev. B **60**, 1953 (1999), and references therein.

[6] The basic idea is to identify a three-level quantum structure: Carriers are injected into the upper level (level three) which is ''metastable'', i.e., weakly coupled to the lower levels; in contrast, carriers in the intermediate level (level two) can relax very fast into the lowest level (level one). As a result, we have $n_3 > n_2$, thus realizing the desired intersubband lasing between levels three and two ($n_3 - n_2 > 0$).

[7] C. Jacoboni and P. Lugli, *The Monte Carlo Method for Semiconductor Device Simulations* (Springer, Wien, 1989).

[8] This is based on a time-step separation between injection/loss and scattering contributions [see Eq. (2)] similar to the generalized MC technique used for the analysis of coherent vs incoherent phenomena in photoexcited semiconductors [T. Kuhn and F. Rossi, Phys. Rev. Lett. **69**, 977 (1992); Phys. Rev. B **46**, 7496 (1992)].

[9] C. Sirtori, P. Kruck, S. Barbieri, P. Collot, and J. Nagle, Appl. Phys. Lett. **73**, 3486 (1998).

[10] For such GaAs-based MQW structure the carrier injection $g_{\mathbf{k}\nu}$ has been modeled in terms of a 3D Fermi–Dirac velocity distribution into level three only [see Eq. (2)] while for the sake of simplicity a **k**-independent loss function Γ_ν has been considered. In our simulation, carriers are injected into level three and extracted from level one with best efficiency. In real structures this injection/loss process strongly depends on the operative conditions (mainly current and temperature) of the device in a nontrivial way. In the present scheme, however, a phenomenological modeling of this dependence would in any case be questionable.

[11] Note the different time scales in Figs. 2(a) and 2(b) which correspond to the different values of the escape time τ_1.

[12] As discussed in Ref. 5, carrier-optical phonon scattering depends strongly on the in-plane momentum transfer.

[13] Contrary to interband gain spectra, we deal with very sharp peaks, whose line width is not affected by in-plane parabolic dispersion.